Atmósfera (1989), **2**, pp. 189-208

On the structure of transient atmospheric waves Part II

A. WIIN-NIELSEN

Geophysical Institute, University of Copenhagen, Denmark

(Manuscript received January 3, 1989; accepted in final form April 6, 1989)

RESUMEN

En esta segunda parte de un estudio de la estructura relativa de las ondas baroclínicas transitorias se presenta un análisis del comportamiento de las ondas en un modelo casi no divergente de 3 capas. Los procedimientos en el análisis son una extensión directa de los usados en la parte I en la que un modelo de 2 capas fue usado. El aumento de trabajo algebraico requerido en el caso de 3 capas se disminuye algo en el dominio complejo con respecto a las fases y amplitudes relativas, manteniendo la misma metodología. Sin embargo, el uso del dominio complejo hace posible obtener los estados estacionarios como las raíces de ecuaciones cúbicas en las que las raíces complejas indican ondas inclinadas. Además, con el nuevo procedimiento, se facilita el análisis de estabilidad de los estados estacionarios derivados.

En vista del descubrimiento de estas ventajas, se consideró que vale la pena reconsiderar el caso de 2 niveles cuando es posible resolver el problema en una forma cerrada en su dependencia en el tiempo (Sección 2).

La Sección 3 que contiene el análisis del caso de los 3 niveles permite no solamente los cambios verticales de estabilidad estática sino también en desviaciones con respecto a un perfil de viento lineal. Mientras que los resultados en el caso de un perfil de viento recto son una extensión natural del caso de 2 niveles. Se encuentra que aumentando los esfuerzos tangenciales negativos del viento en la capa superior, desestabilizará las soluciones de estado estacionario.

ABSTRACT

In this second part of a continuing study of the relative structure of transient baroclinic waves an analysis of the behavior of waves in a three-level, quasi-nondivergent model is presented. The procedures applied in the analysis are a straightforward expansion of those used in Part I in which the two-level model was used.

The increased algebraic work required by the three level case is eased somewhat by working in the complex domain with respect to the relative amplitudes and phases, but otherwise the methodology is maintained. However, the use of the complex domain makes it possible to obtain the steady states as the roots to cubic equations where complex roots indicate sloping waves. In addition, the stability analysis of the derived steady states goes easier in the new procedure. In view of the discovery of these advantages it was considered worthwhile to reconsider the two-level case where it is possible to solve the time-dependent problem in a closed form (section 2).

Section 3 contains the analysis of the three-level case permitting not only vertical changes of the static stability but also deviations from a linear windprofile. While the results in the case of a straight windprofile are a natural extension of the two-level case, it is found that increasing negative windshears in the upper layer will destabilize the steady state solutions.

1. Introduction

The structure of transient baroclinic waves in a two-level, quasi-nondivergent model was investigated by the author (1989), hereafter refered to as I. The procedure was to use the vertical mean flow as a reference and to investigate the amplitude and the vertical slope relative to the wave in the mean flow which in this simple model is at the 50 kPa level. Time-dependent equations for the relative amplitude and the relative phase were derived, stationary states were determined, and the stability of these states were decided by linear perturbation analysis.

While the two-level model applied in the above study contains the essentials of large-scale dynamics it is also somewhat restricted because only linear profiles of the basic zonal winds are permitted, and a single standard value of the static stability factor is used. It is thus desirable to expand the study to include a higher vertical resolution. In this paper we shall extend the study to the three-level model which permits two static stabilities and can distinguish between different windshears in the lower and the upper half of the atmosphere.

However, before we turn on attention to the three-level model, we shall, in section 2, briefly return to the two-level model. The reason is that it turns out that the stability investigation of the steady states is unnecessary because the time-dependent equations can be solved directly in a closed form.

2. The two-level model, revisited

In I there is a detailed description of the application of the two-level model in the determination of the relative structure of the transient baroclinic wave. The most important equations describe the time-dependent behavior of the relative amplitude, r and the relative phase, ϕ. The following quantities enter in the equation:

$k = 2\pi/L$, k is the wave number, L the wavelength, U_T, the thermal wind,

$C_R = \beta/k^2$, C_R, the Rossby velocity, β the Rossby parameter,

$q^2 = 2f_o^2/(\sigma P^2)$, f_o, a standard value of the Coriolis parameter, $P = 50\ kPa$, $\sigma = -\alpha\partial ln\theta/\partial p$, α, the specific volume, θ, the potential temperature, p, the pressure, $\lambda^2 = q^2/k^2$

The two equations are:

$$\frac{dr}{dt} = kU_T[\frac{\lambda^2 - 1}{\lambda^2 + 1} - r^2]\ \sin\ \phi$$

$$r\frac{d\phi}{dt} = kU_T[\frac{\lambda^2 - 1}{\lambda^2 + 1} + r^2]\ \cos\ \phi - \frac{\lambda^2}{\lambda^2 + 1}C_R r \tag{2.1}$$

Replacing the determination of the stationary states of the system (2.1) and their stability we propose to solve the system (2.1) directly. This can be done by introducing first the quantities

$$x = r\ \cos\ \phi,\ \ y = r\ \sin\ \phi \tag{2.2}$$

giving the equations

$$\frac{dx}{dt} = -2kU_T xy + kC_R\frac{\lambda^2}{\lambda^2 + 1}y$$

$$\frac{dy}{dt} = kU_T(x^2 - y^2) - kC_R\frac{\lambda^2}{\lambda^2 + 1}x + kU_T\frac{\lambda^2 - 1}{\lambda^2 + 1} \tag{2.3}$$

An inspection of (2.3) shows that it is advantageous to introduce the complex variable

$$z = x + iy \tag{2.4}$$

resulting in the simple equation

$$\frac{dz}{dt} = ikU_T[z^2 - \frac{\lambda^2}{\lambda^2+1}\frac{C_R}{U_T}z + \frac{\lambda^2-1}{\lambda^2+1}] \tag{2.5}$$

(2.5) is easily solved by separation of variables. We may write the solution in the form:

$$\frac{z-z_+}{z-z_-} = \frac{z(0)-z_+}{z(0)-z_-} \exp\ (ikU_T(z_+ - z_-)t) \tag{2.6}$$

in which $z(0)$ is the initial value and

$$z_+ = z(r) + iz(i)$$

$$z_- = z(r) - iz(i)$$

with

$$z(r) = \frac{1}{2}\frac{\lambda^2}{\lambda^2+1}\frac{C_R}{U_T} \tag{2.8}$$

$$z(i) = [\frac{\lambda^2-1}{\lambda^2+1} - z(r)^2]^{\frac{1}{2}} \tag{2.9}$$

We notice from the solution (2.6) that it satisfies the requirement $z = z(0)$ for $t = 0$.

We remark also that $z_+ - z_- = 2iz(i)$ indicating that the argument in the exponential function is real and negative provided $U_T > 0$, which means that the wind in the basic state is increasing with height. This means also that the exponential function goes to zero as t goes to infinity. It follows that z approaches z_+ in the same limit regardless of the initial state. On the other hand if $U_T < 0$ it is seen from (2.6) that z will tend to z_- for t going to infinity. It should of course be stressed that we have only considered the case in which the roots, corresponding to the steady states, are complex. In the case of real roots, considered in I, we got an oscillatory motion from (2.5).

For the sake of completeness we shall point out that z_+ corresponds to a wave in which the thermal wave is lagging behind the wave in the vertical mean flow, since both $z(r)$ and $z(i)$ are positive. We have therefore

$$\psi_{Tr}(x) = z(r)\ \cos\ kx - z(i)\ \sin\ kx = r_a\ \cos\ (kx + \phi_a) \tag{2.10}$$

with

$$r_a = (z(r)^2 + z(i)^2)^{\frac{1}{2}} \text{ and } \phi_a = \text{ arc } \tan(z(i)/z(r)) > 0$$

From (2.10) it is seen that the ridge in the thermal field is located at a negative value of x while the ridge in the reference field by definition is located at $x = 0$.

It may be instructive to consider some examples of how the wave from a given initial state approach the stable steady state z_+. The various cases are obtained from (2.6) by solving for z and calculating $z(t)$.

Fig. 1 comes from a case where the initial state is $z(0) = (0,\ 0)$ corresponding to zero amplitude in the initial state. This means that the initial state is equivalent barotropic. The trajectory $z(t)$, calculated with marks for every half day shows that the stable steady state for practical purposes is reached in 4 days with the thermal field gradually falling behind the 50 kPa field (ϕ positive). In this and the following cases the values of $U_T = 20\ \mathrm{ms}^{-1}$ and $L = 4 \times 10^6\mathrm{m} = 4000$ km have been used.

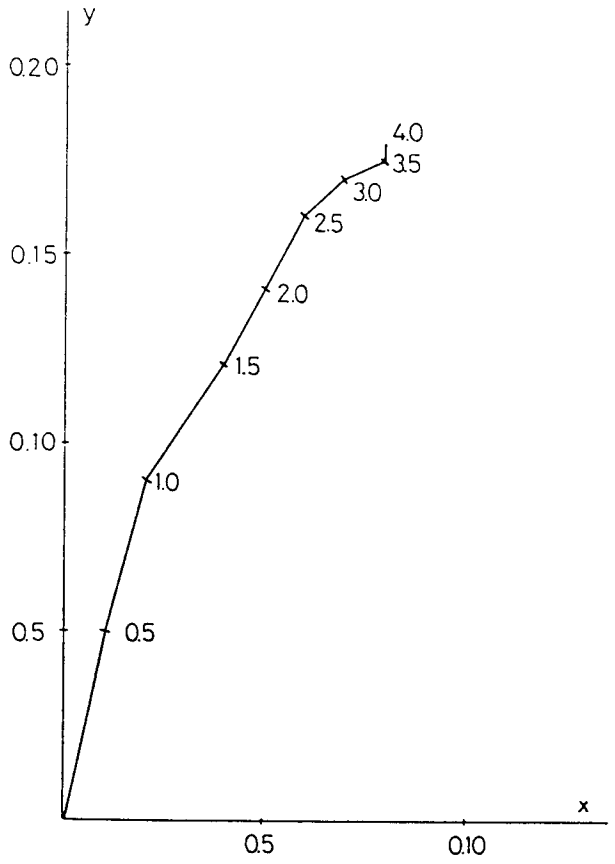

Fig. 1. The trajectory of a relative wave from the initial state (0, 0) to the stable steady state (marked by a circle). The marks indicate time in days. ($U_T = 20\ \mathrm{ms}^{-1}$, $L = 4 \times 10^6$ m).

The next case is one in which the initial value of $z(0)$ is selected close to z_-, i.e., the unstable stationary state which is (0.08, -0.18). The first starting point is (0.08, -0.17). From here ϕ increases steadily until the state (0.08, 0.18) is reached. On the other hand, with a starting point at (0.08, -0.19) we find that the trajectory $z(t)$ goes the opposite way around approaching the stable steady state from the opposite direction. Similar long trajectories can be obtained for other starting positions as shown in Fig. 3 where the initial state is (1, -1).

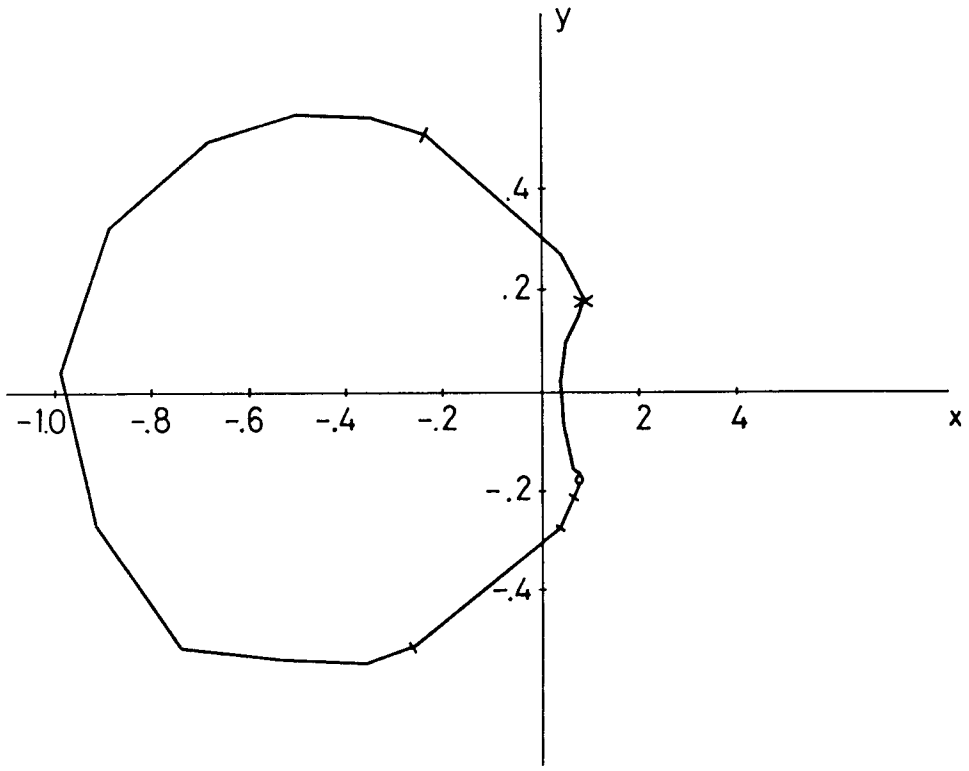

Fig. 2. The trajectories starting close to the unstable steady state, marked by a circle, and both ending in the stable steady state, marked by a cross. ($U_T = 20$ ms^{-1}, $L = 4 \times 10^6$ m).

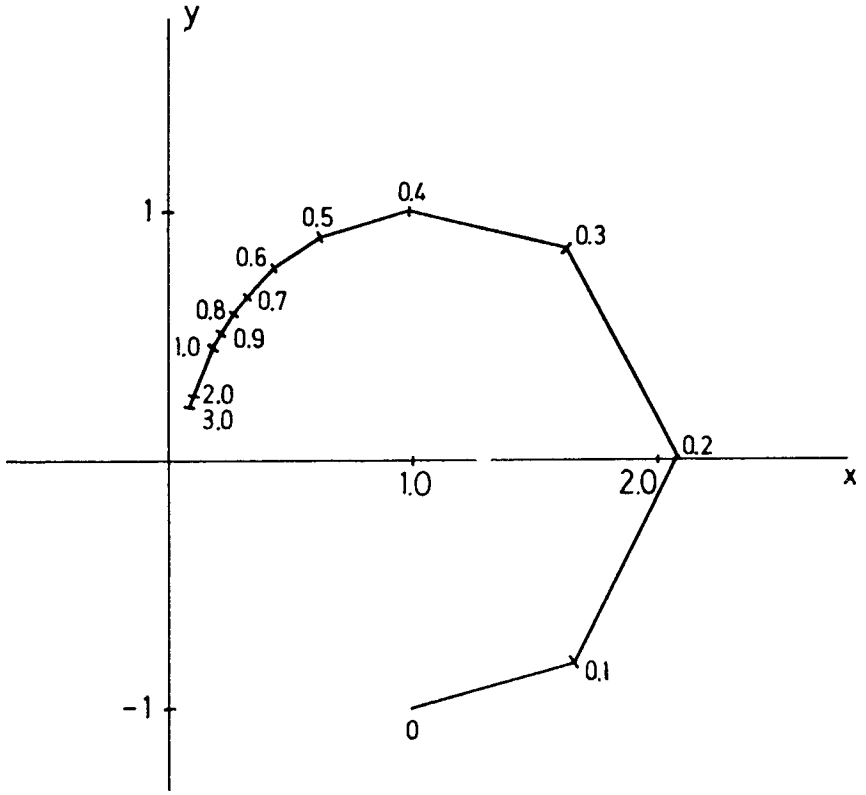

Fig. 3. As Fig. 1 with start in (1, -1).

Quite large values of $r(t)$ can be obtained in this adjustment to the stable steady state. An example with the initial value (0, -1) is shown in Fig. 4. The starting point correspond to a relative amplitude of 1 and a situation where the thermal field is 90° ahead of the geopotential field. The relative amplitude attains values as large as 11.5 at a time when the thermal field and the 50 kPa geopotential differ by half a wavelength. Note, also that the first part of the process goes fast, while the final approach to the stable steady state is considerably slower.

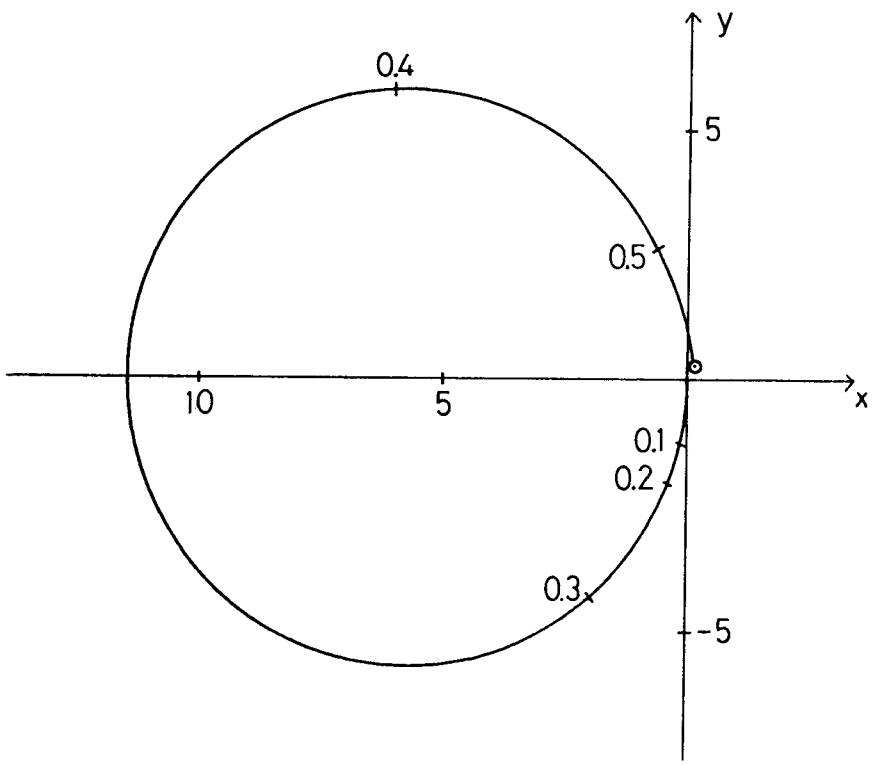

Fig. 4. As Fig. 1 with start in (0, -1).

3. The three-level model

The quasi-nondivergent, three-level model has been described in several papers (Charney and Phillips, 1953; Cressman, 1961 and Wiin-Nielsen, 1961). It represents the lowest vertical resolution which permits deviations from a linear windprofile in the basic state and a vertical variation of the static stability parameter. It is therefore worthwhile to study the expansion of the procedures used in I to this somewhat more general case. In view of the earlier treatments of the model it will suffice to give the equations for the model and explain the notations. We shall use seven vertical levels denoted by subscripts: 0, 1, · · , 6. The corresponding values of pressure are $(i/6)p_o$, with $p_o = 100$ kPa and $i = 0, 1, \cdots, 6$. We introduce also the subscripts:

$$( )_T = ( )_1 - ( )_3$$

$$( )_B = ( )_3 - ( )_5 \tag{3.1}$$

Otherwise the notations are the same as in section 2 and in I.

The basic equations are the quasi-nondivergent vorticity equation applied at levels 1, 3 and 5 and the thermodynamic equation applied at levels 2 and 4. It is assumed that the boundary conditions are $\omega_o = 0$ and $\omega_6 = 0$, and that heating and friction are neglected. The two thermodynamic equations at levels 2 and 4 are used to eliminate the vertical velocities appearing in the vorticity equations. As a final step we used (3.1) to form two thermal vorticity equations, one for the layer between levels 1 and 3, and one for the layer between levels 3 and 5. The result is the following set of three equations:

$$\frac{\partial}{\partial t}[\zeta_T - 2q_2^2\psi_T + q_4^2\psi_B] + V_3 \bullet \nabla[\zeta_T - 2q_2^2\psi_T + q_4^2\psi_B] + V_T \bullet \nabla(\zeta_3 + \zeta_T) + \beta V_T = 0$$

$$\frac{\partial}{\partial t}[\zeta_B - 2q_4^2\psi_B + q_2^2\psi_T] + V_3 \bullet \nabla[\zeta_B - 2q_4^2\psi_B + q_2^2\psi_T] + V_B \bullet \nabla(\zeta_3 - \zeta_B) + \beta V_B = 0$$

$$\frac{\partial}{\partial t}[\zeta_3 - q_4^2\psi_B + q_2^2\psi_T] + V_3 \bullet \nabla[\zeta_3 - q_4^2\psi_B + q_2^2\psi_T] + \beta V_3 = 0 \tag{3.2}$$

In the calculation of the coefficients in (3.2) it is necessary to specify the static stability at levels 2 and 4. This is done by assuming that the layer below level 3 (50 kPa) has a constant lapse rate γ_B, while the layer above level 3 is characterized by the lapse rate γ_T. For a layer with a constant lapse rate it can be shown (Jacobs and Wiin-Nielsen, 1966) that

$$\sigma = -\frac{\alpha}{\theta}\frac{\partial\theta}{\partial p} = \frac{R^2T_o}{gp_o^2}(\gamma_d - \gamma)\left[\frac{p}{p_o}\right]^{-(2-R\gamma/g)} \tag{3.3}$$

where R is the gas constant, g the acceleration of gravity, γ_d the dry adiabatic lapse-rate and T_o and p_o the temperature and the pressure at the bottom of the layer. With these assumptions one may calculate σ_4 and σ_2 with the result that

$$\sigma_4 = \frac{R^2T_0}{gp_0^2}(\gamma_d - \gamma_B)\left[\frac{p^4}{p_0}\right]^{-(2-R\gamma_B/g)} \tag{3.4}$$

and

$$\sigma_2 = \frac{R^2T_0}{gp_0^2}(\gamma_d - \gamma_T)\left[\frac{p^2}{p_0}\right]^{-(2-R\gamma_T/g)} \bullet \left[\frac{p_3}{p_0}\right]^{R(\gamma_B-\gamma_T)/g} \tag{3.5}$$

One may then proceed to calculate

$$q^2 = \frac{2f_0^2}{\sigma P^2} \tag{3.6}$$

at the levels 2 and 4, and from these the two parameters

$$\lambda_2^2 = \frac{q_2^2}{k^2};\quad \lambda_4^2 = \frac{q_4^2}{k^2} \tag{3.7}$$

The disturbances to be introduced in (3.2) shall have the form

$$\psi = \hat{\psi}(t) \exp(ikx) \tag{3.8}$$

(3.8) with the proper subscripts are substituted in (3.2). It is then a straightforward matter to determine equations which contain the time-derivatives of $\hat{\psi}_3$, $\hat{\psi}_T$ and $\hat{\psi}_B$. These equations are linear, and by a simple solution for the three time-derivatives we obtain the following equations

$$\frac{d\hat{\psi}_T}{dt} = -ik[g_3\hat{\psi}_3 + g_T\hat{\psi}_T - g_B\hat{\psi}_B]$$

$$\frac{d\hat{\psi}_B}{dt} = -ik[h_3\hat{\psi}_3 - h_T\hat{\psi}_T + h_B\hat{\psi}_B]$$

$$\frac{d\psi_3}{dt} = -ik[s_3\hat{\psi}_3 - s_T\hat{\psi}_T + s_B\hat{\psi}_B] \tag{3.9}$$

in which the nine coefficients are expressed in the parameters of the problem, i.e., U_3, U_T, U_B, λ_2^2 and λ_4^2. The details are given later in this section.

We continue the development in analogy with the procedures used in I, and the next step is to obtain the equations for the rate of change of the amplitudes. These are most easily obtained by noting that the following relation holds:

$$\hat{\psi} \bullet \tilde{\psi} = \frac{1}{2}(A - iB) \bullet \frac{1}{2}(A + iB) = \frac{1}{4}R^2 \tag{3.10}$$

where (˜) indicates the complex conjugate.

It is thus straightforward to derive equations for dR/dt by finding the complex conjugates of the three equations (3.9) and proceed in accordance with (3.10). The result is

$$\frac{dR_T}{dt} = -k[g_3R_3 \sin \delta_T + g_BR_B \sin (\delta_B - \delta_T)]$$

$$\frac{dR_B}{dt} = -k[h_3R_3 \sin \delta_B - h_TR_T \sin (\delta_B - \delta_T)]$$

$$\frac{dR_3}{dt} = -k[s_TR_T \sin \delta_T - s_BR_B \sin \delta_B] \tag{3.11}$$

in which the relative phase δ is defined by

$$\delta = \theta_3 - \theta \tag{3.12}$$

where θ is the absolute phase angle.

To close the system it is necessary to obtain equations for the rate of change of the phase angles.

Using the expression for ψ and its complex conjugate (see 3.10) we obtain that

$$\tan\ \theta = i\frac{\hat{\psi} - \tilde{\psi}}{\hat{\psi} + \tilde{\psi}} \tag{3.13}$$

From (3.13) we obtain by differentiation with respect to time

$$R^2\frac{d\theta}{dt} = 2i[\tilde{\psi}\frac{d\hat{\psi}}{dt} - \hat{\psi}\frac{d\tilde{\psi}}{dt}] \tag{3.14}$$

Using (3.14), (3.9) and the complex conjugates we obtain:

$$R_T^2 = \frac{d\theta_T}{dt} = k[g_3R_3R_T\ \cos\ \delta_T + g_TR_T^2 - g_BR_TR_B\ \cos\ (\delta_B - \delta_T)]$$

$$R_B^2\frac{d\theta_B}{dt} = k[h_3R_3R_B\ \cos\ \delta_B - h_TR_TR_3\ \cos\ (\delta_B - \delta_T) + h_BR_B^2]$$

$$R_3^2\frac{d\theta_3}{dt} = k[s_3R_3^2 - s_TR_TR_3\ \cos\ \delta_T + s_BR_BR_3\ \cos\ \delta_B] \tag{3.15}$$

Still following the analogy to I we introduce the quantities

$$r_T = \frac{R_T}{R_3};\ r_B = \frac{R_B}{R_3};\ \delta_T = \theta_3 - \theta_T;\ \delta_B = \theta_3 - \theta_B \tag{3.16}$$

It is then possible to obtain the equations for the rate of change of the two relative phases by combining (3.11), (3.15) and (3.16). We get:

$$\frac{dr_T}{dt} = k[(s_Tr_T^2 - g_3)\ \sin\ \delta_T - s_Br_Br_T\ \sin\ \delta_B - g_Br_B\ \sin\ (\delta_B - \delta_T)]$$

$$r_T\frac{d\delta_T}{dt} = k[-(s_Tr_T^2 + g_3)\ \cos\ \delta_T + s_Br_Br_T\ \cos\ \delta_B + g_Br_B\ \cos\ (\delta_B - \delta_T) + C_Tr_T] \tag{3.17}$$

$$\frac{dr_B}{dt} = k[s_Tr_Br_T\ \sin\ \delta_T - (s_Br_B^2 + h_3)\ \sin\ \delta_B + h_Tr_T\ \sin\ (\delta_B - \delta_T)]$$

$$r_B\frac{d\delta_B}{dt} = k[-s_Tr_Br_T\ \cos\ \delta_T + s_Br_B^2 - h_3)\ \cos\ \delta_B + h_Tr_T\ \cos\ (\delta_B - \delta_T) + C_Br_B]$$

in which

$$C_T = s_3 - g_t,\ C_B = s_3 - h_3 \tag{3.18}$$

It is possible to solve for the steady states of (3.17) as the system is formulated, but the calculations are rather cumbersome. We shall therefore follow the same ideas as with the two level model and

consider the two complex numbers

$$Z_B = x_B + iy_B = r_B \cos \delta_B + ir_B \sin \delta_B$$

$$Z_T = x_T + iy_T = r_T \cos \delta_T + ir_T \sin \delta_T \tag{3.19}$$

Using these definitions and the system (3.17) we may by elementary derivations obtain the following two equations

$$\frac{dZ_T}{dt} = ik[C_T Z_T + s_T Z_T^2 - g_3 + s_B Z_T Z_B + g_3 Z_B]$$

$$\frac{dZ_B}{dt} = ik[C_B Z_B + s_B Z_B^2 - h_3 + s_T Z_T Z_B - h_T Z_T] \tag{3.20}$$

where the constants are defined in the following way:

$$\Delta = (1 + 2\lambda_2^2)(1 + 2\lambda_4^2) - \lambda_2^2\lambda_4^2$$

$$\Delta \bullet C_T = [2\lambda_2^2(1 + \lambda_4^2) - (1 + 2\lambda_4^2)]U_T - 2\lambda_4^2(1 + \lambda_2^2)U_B$$

$$\Delta \bullet C_B = 2\lambda_2^2(1 + \lambda_4^2)U_T - [2\lambda_4^2(1 + \lambda_2^2) - (1 + 2\lambda_2^2)]U_B$$

$$\Delta \bullet s_T = \lambda_2^2(1 + \lambda_4^2)U_T; \quad \Delta \bullet g_B = \lambda_4^2 U_B$$

$$\Delta \bullet s_B = \lambda_4^2(1 + \lambda_2^2)U_B; \quad \Delta \bullet h_T = \lambda_2^2 U_T$$

$$\Delta \bullet g_3 = [(1 - 2\lambda_2^2)(1 + 2\lambda_4^2) + \lambda_2^2\lambda_4^2]U_T + Z\lambda_4^2 U_B$$

$$\Delta \bullet h_3 = [(1 + 2\lambda_2^2)(1 - 2\lambda_4^2) + \lambda_2^2\lambda_4^2]U_B + 2\lambda_2^2 U_T \tag{3.21}$$

It would naturally be desirable to solve the two coupled differential equations in (3.20) in a closed form, but a method of solution is unknown to the author. However, it is possible to find the steady states of these equations. We may then afterwards determine the stability of the various steady states. This procedure will lead to a cubic equation for the steady states obtained by eliminating one of the variables from the two equations for the steady states. For example, we may decide to eliminate Z_T. Since the second steady state equation is linear in Z_T we find

$$Z_T = \frac{C_B Z_B + s_B Z_B^2 - h_3}{h_T - s_T Z_B} \tag{3.22}$$

This equation for Z_T is introduced in the steady state equation obtained from the first equation

in (3.20). After evaluation we obtain the cubic equation:

$$A_3 Z_B^3 + A_2 Z_B^2 + A_1 Z_B + A_o = 0 \tag{3.23}$$

with

$$A_3 = s_T s_B (C_B - C_T) + g_B s_T + h_{T1} s_B^2$$

$$A_2 = h_T s_B (C_B + C_T) - h_3 s_T s_B + s_T C_B^2 - g_3 s_T^2 - s_T (C_B C_T + 2 g_3 h_T)$$

$$A_1 = C_T (h_T C_B + s_T h_3) + 2 S_T (g_3 h_T - C_B h_3) + h_T (g_B h_T - s_B h_3)$$

$$A_o = s_T h_3^2 - C_T h_T h_3 - g_3 h_T^2 \tag{3.24}$$

The solutions of (3.23) are obtained by using the classical formulas for the cubic equation. It is seen that we shall in general obtain three values of Z_B, of which one will be real because the coefficients A_i all are real. To the real value of Z_B corresponds a real value of Z_T obtained from (3.22), while complex values of Z_B in general will give complex values of Z_T.

The next question is the stability of the computed steady states which we shall denote with an overbar. Let $\overline{Z}_B$, $\overline{Z}_T$ be an arbitrary steady state. The linearized perturbation equations are then:

$$\frac{dZ_T'}{dt} = ik[(C_T + 2 s_T \overline{Z}_T + s_B \overline{Z}_B) Z_T, \; + (s_B \overline{Z}_T + g_B) Z_B']$$

$$\frac{dZ_B'}{dt} = ik[(s_T \overline{Z}_B - h_T) Z_T' + (C_B + 2 s_B \overline{Z}_B + s_T \overline{Z}_T) Z_B'] \tag{3.25}$$

The perturbations, denoted by a prime, will be of the form

$$Z_T' = \hat{Z}_T \exp(-i\nu t), \; Z_B = \hat{Z}_B \exp(-i\nu t) \tag{3.26}$$

With the assumption (3.26) for the perturbations it is seen that if ν is complex with a positive real part we shall have instability because

$$\exp(-i(\nu_r + i\nu_i)t) = \exp(\nu_i t) \exp(-i\nu_r t) \tag{3.27}$$

Otherwise, the eigenvalue problem presented by (3.25) is a standard problem leading to a quadratic equation in ν which may be solved directly.

Regarding the interpretation of the results we are helped by the fact that the two solutions to (3.23) which may be complex are also complex conjugates. This means that r_B is the same for the two solutions while the phase angle δ_B is numerically the same, but the signs are opposite. It is also seen from (3.22) that if Z_B is replaced by its complex conjugate then Z_T will be exchanged with its complex conjugate.

4. Results

The equations derived in the previous section have been used to calculate some examples of the vertical structure of baroclinic waves in their relative steady state together with an investigation of the stability of the steady states. The procedure starts with a solution of (3.23) giving Z_B as the three roots of the cubic equation. For each Z_B we obtain Z_T from (3.22). The stability of a given steady state may then be obtained from calculating the eigenvalues from (3.25). The expression (3.27) shows that if the eigenvalue is real we shall have a neutral stability connected with an oscillatory solution, while $\nu_i > 0$ indicates instability and $\nu_i < 0$ stability. Note, that while the solutions for Z_B and Z_T come in conjugate pairs, this is not the case for the frequencies determined as eigenvalues from (3.25) because the coefficients are complex in this case. For stability it is thus necessary to require that the imaginary parts of both solutions are negative, while a single positive value of ν_i indicates instability.

Fig. 5 shows the relative phases δ_1 and δ_5 for wavelengths less than 12000 km for a case with $U_B = U_T = 15$ ms^{-1} and $\gamma_B = \gamma_T = 6.5 \times 10^{-3}$ km^{-1}. This case corresponds to a low order representation of the Charney-solution (1947). The figure indicates that sloping waves are present as stationary states for 3000 km $\leq L \leq$ 11000 km. The other solution will have the opposite signs of both δ_1 and δ_5. However, the solution shown is the westward sloping solution because $\delta_5 > 0$ and $\delta_1 < 0$. A typical slope for, say, $L = 5000$ km is about 1.3 rad or 75° corresponding to 20% of the wavelength. It can also be seen that the slopes become larger than a quarter of a wavelength for the

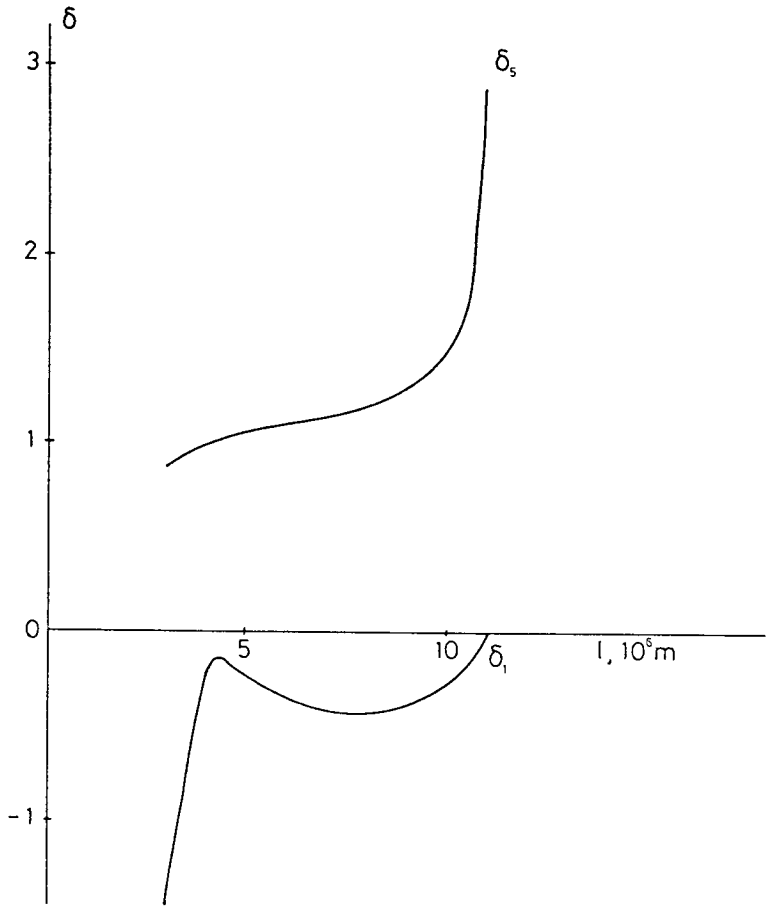

Fig. 5. The relative phase-angles (δ_1 and δ_5) as a function of wavelength, measured in 10^6 m, for $U_B = U_T = 15$ ms^{-1} and $\gamma_B = \gamma_T = 6.5 \times 10^{-3}$ km^{-1}.

short and the long wave part of the interval. Fig. 6 shows the corresponding relative amplitudes r_1 and r_5. For short waves we find the larger relative amplitude at the lower level (i.e., $r_5 > r_1$) while the opposite is the case for long waves. The imaginary parts of the two frequencies can be seen in Fig. 7 using a unit of days^{-1}. We note that the structures shown in the two previous figures are stable for 3000 km $\leq L \leq$ 8800 km. This result shows that with the additional degree of freedom in a three-level model as compared to a two-level model we cannot necessarily conclude that a west-ward sloping wave as a stationary state is also stable.

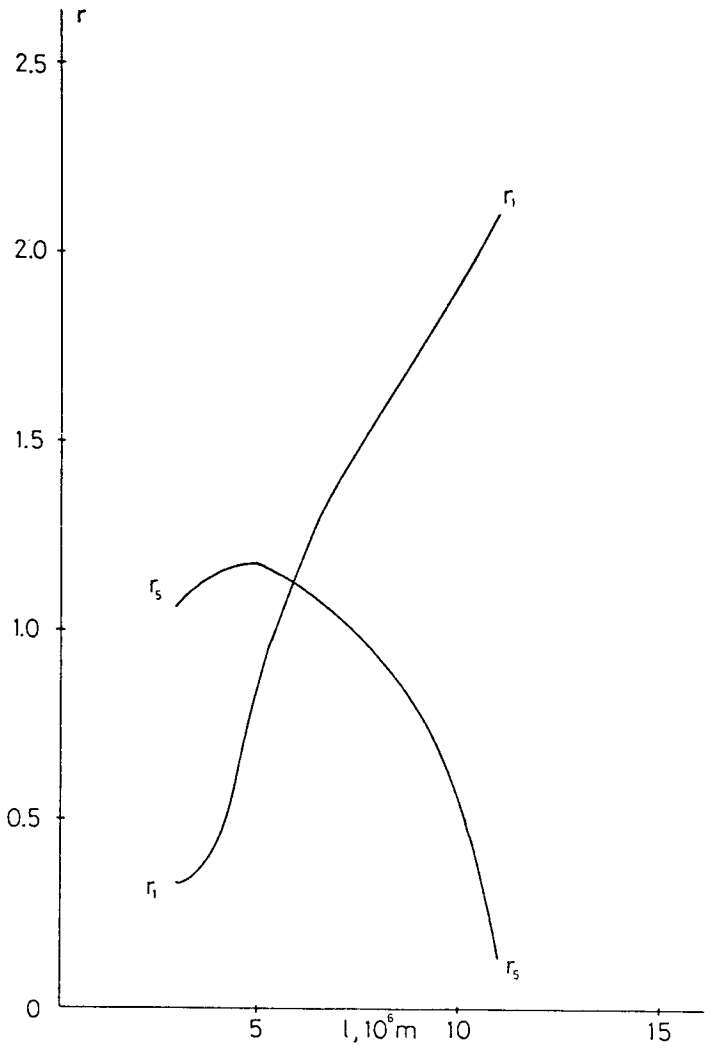

Fig. 6. The relative amplitudes (r_1 and r_5) as a function of wavelength for the case in Fig. 5.

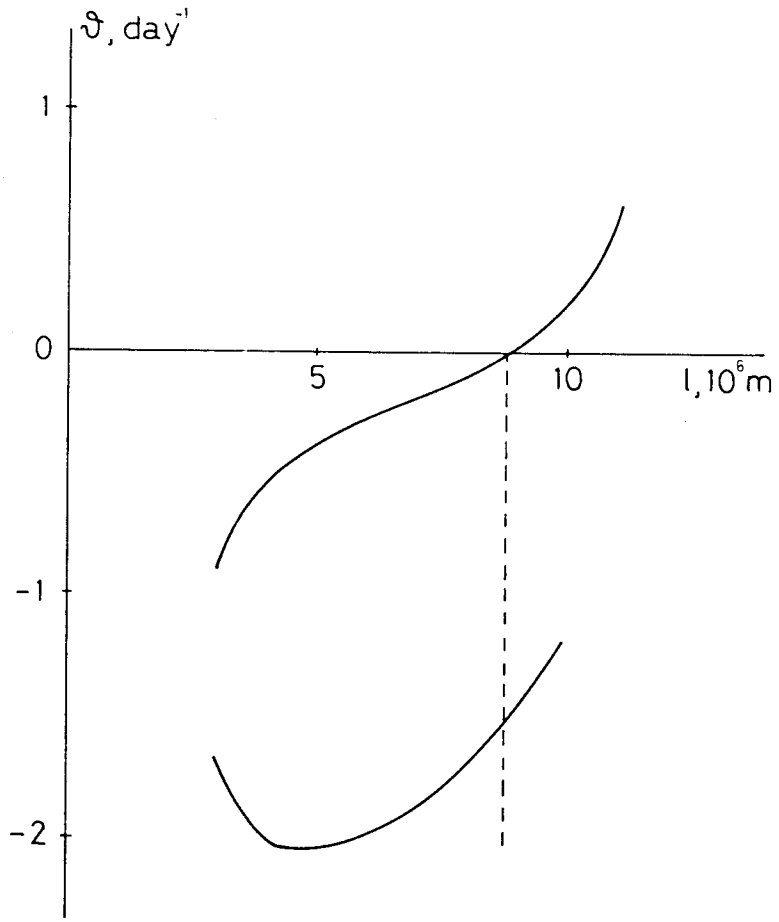

Fig. 7. The two frequencies measured in days^{-1} as a function of wavelength for the case in Fig. 5.

In addition to the waves described in Figs. 5-7 it turns out that the sloping waves are present also for 14000 km $\leq L \leq$ 28000 km. The limit of 28000 km is selected because the number is approximately the length of the 45° parallel. Fig. 8 shows the phase angles for the west-ward sloping wave. The slope is quite large, almost half a wave length in most cases, which is in agreement with observations for the transient very long waves. The relative amplitudes are given in Fig. 9 where the values at level 1 in all cases are larger than at level 5. Finally, Fig. 10 shows that these configurations are stable.

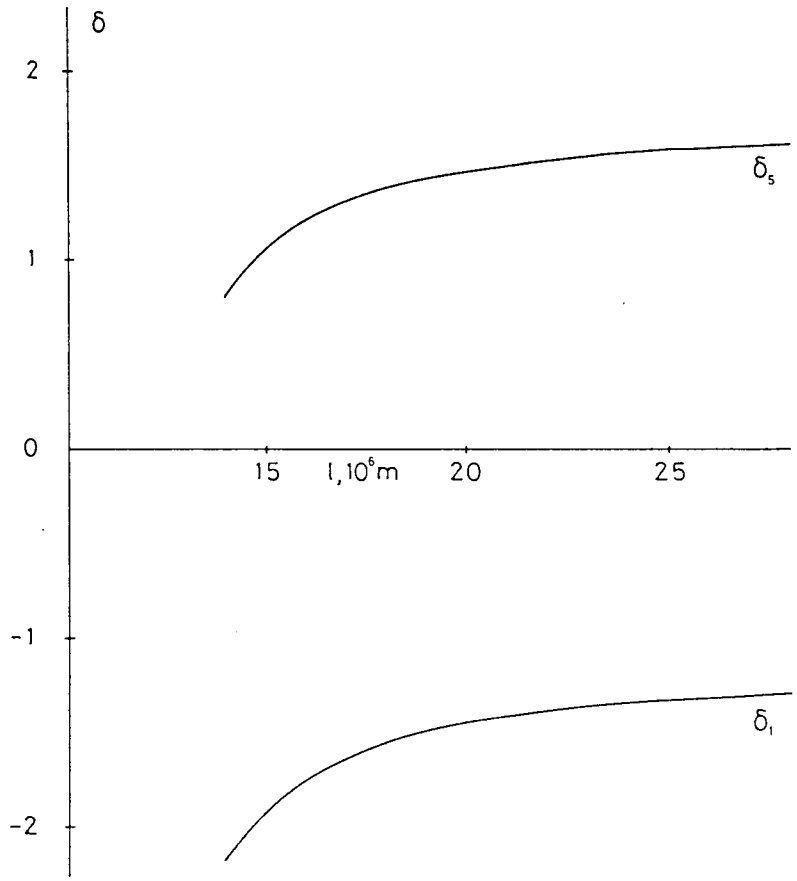

Fig. 8. As Fig. 5, but for wavelengths larger than 10000 km.

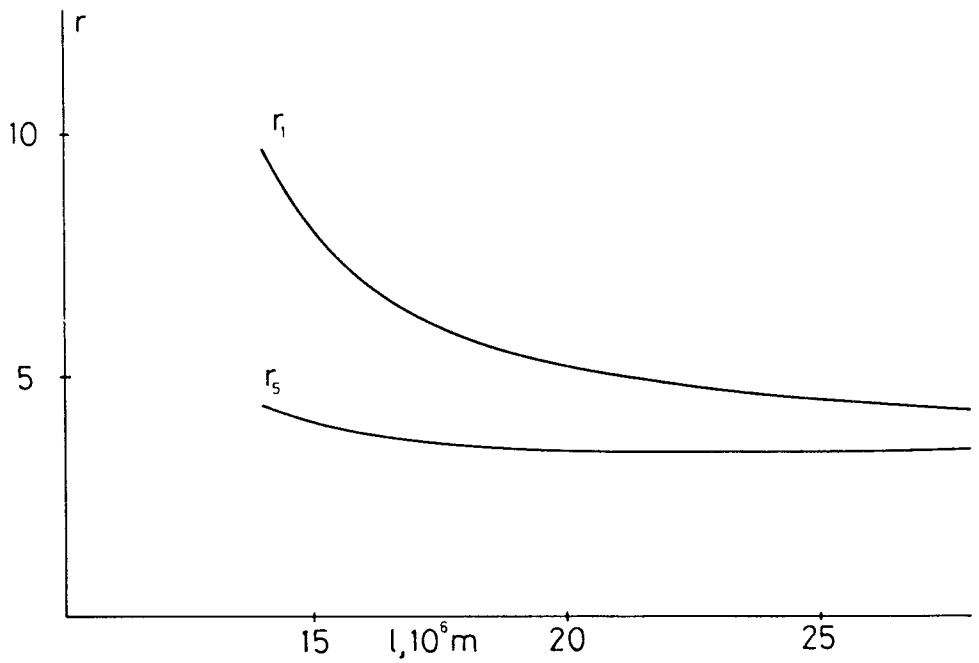

Fig. 9. As Fig. 6, but for wavelengths larger than 10000 km.

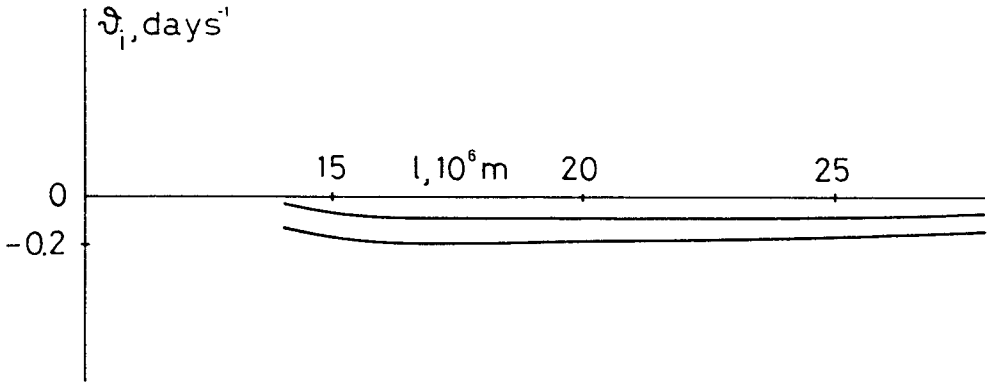

Fig. 10. As Fig. 7, but for wavelengths larger than 10000 km.

In the next series of calculations we have kept the wavelength constant at $L = 5 \times 10^6$m. Similarly $U_B = 15$ ms^{-1} in all calculations while U_T has been varied from -30 ms^{-1} to +30 ms^{-1} with an interval of 5 ms^{-1} With this arrangement we find that the wave at level 5 is in front of the wave at level 3 in all cases, or, in other words, the wave is sloping westward in the lower part of the atmosphere. The westward slope is continued in the upper layer as long as $U_T \geq -5$ ms^{-1}. However, for $U_T < -5$ ms^{-1} the slope in the upper layer is eastward reaching quite larger values when U_T is negative and numerically large. Fig. 11 shows δ_1 and δ_5 as a function of U_T, and it is on the basis of this figure that the description above has been given.

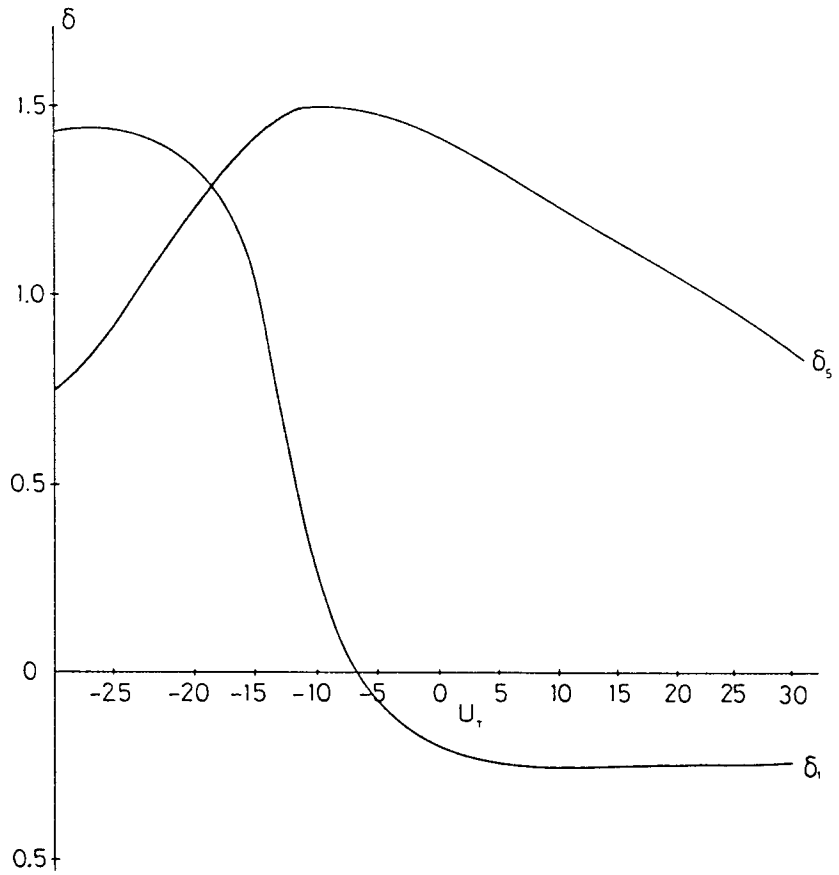

Fig. 11. The relative phase-angles (δ_1 and δ_5) as a function of the windshear U_T in the upper layer with $U_B = 15$ ms^{-1} and $L =$ 5000 km.

We turn next to the relative amplitudes. Fig. 12 shows r_1 and r_5 as functions of U_T in an arrangement similar to Fig. 11. As we can see from Fig. 6 $r_5 > r_1$ for $L = 5 \times 10^6$ m where $U_B = U_T = 15$ ms^{-1}. This relationship holds as long as $U_T \geq 15$ ms^{-1}, but if $U_T < -15$ ms^{-1} we have $r_1 > r_5$.

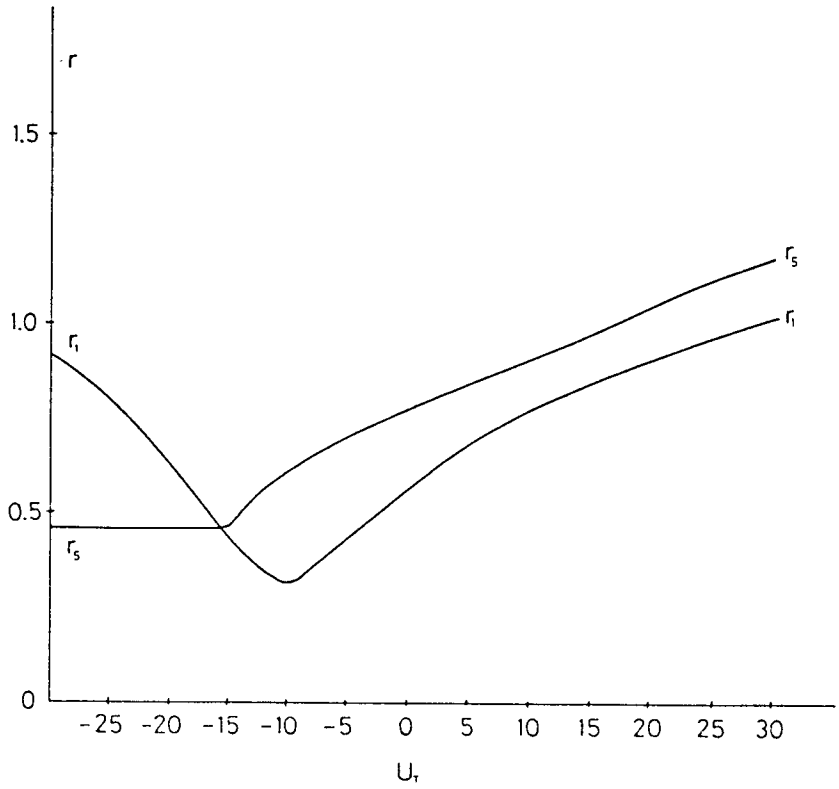

Fig. 12. The relative amplitudes (r_1 and r_5) as a function of U_T for $U_B = 15$ ms^{-1} and $L = 5000$ km.

The structures shown in Figs. 11 and 12 are steady states. In Fig. 13 we show the imaginary part of the frequencies. As we recall, both of these frequencies have to be negative to secure the stability of the steady state. It is seen that the states with $U_T < 5$ ms^{-1} are unstable, while the stationary states with $U_T \geq 10$ ms^{-1} are stable.

The wavelength used in Figs. 11 to 13 is a typical scale for baroclinic disturbances. The main conclusion is that large negative values of U_T will destroy the stability of the steady states. We may investigate this statement for other wavelengths. In Fig. 14 is shown the regions in the (L, U_T)-plane in which a stable relative steady state is found. We notice two regions. For the standard baroclinic waves (2000 km $< L <$ 8000 km) we find a band of wavelengths (2000 km $< L <$ 4000 km) where stable steady states are found for all values of U_T, i.e., - 30 ms^{-1} $\leq U_T \leq$ 30 ms^{-1}. For 4000 km $< L <$ 7500 km we see the destabilizing effects of the negative wind shear, and in the upper part of this interval only large positive values of U_T will result in stable structures. Another region of stable structures are found for $L >$ 8000 km, but also here we notice the effect of numerically large, but negative values of U_T. Note, that the stable steady states in Fig. 14 do not necessarily have a westward slope.

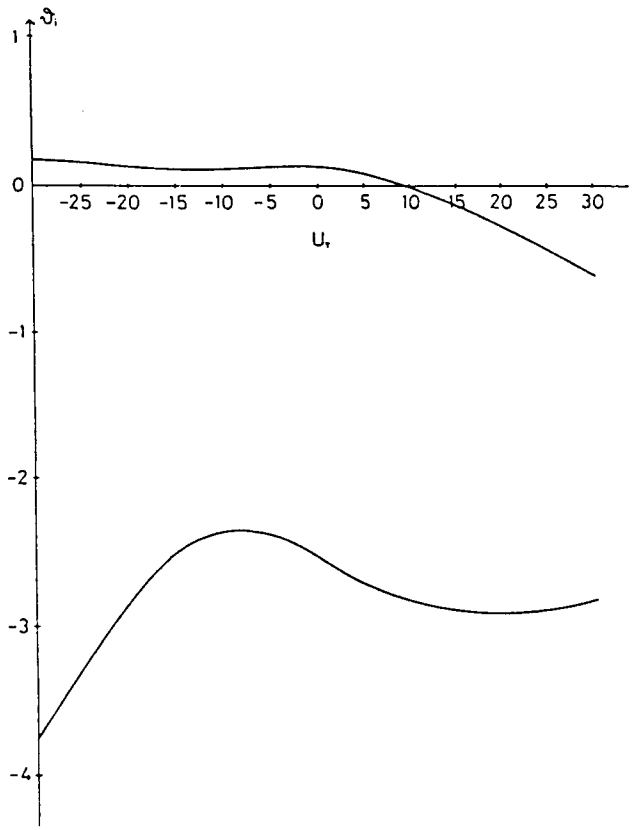

Fig. 13. The two frequencies as a function of U_T for $U_B = 15$ ms^{-1} and $L = 5000$ km.

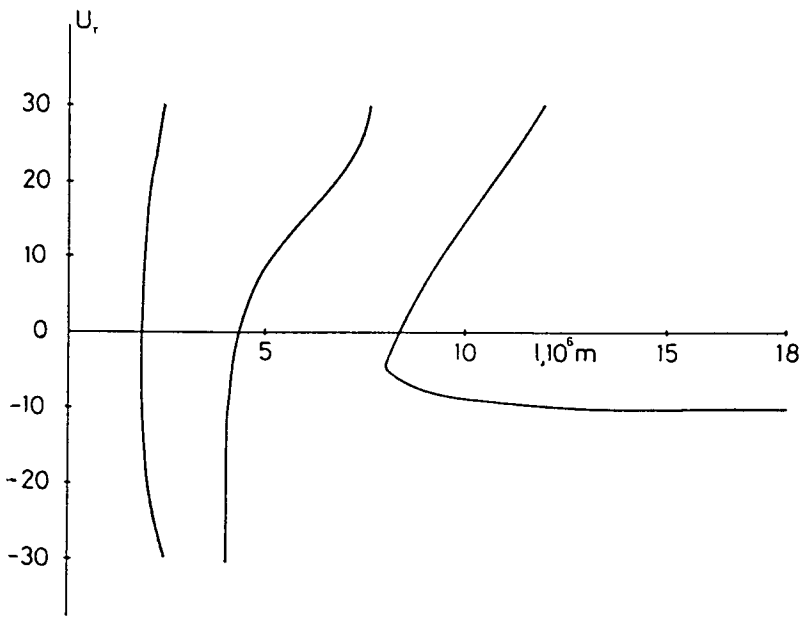

Fig. 14. In the (L, U_T)-diagram are shown the regions of stable steady states for $U_B = 20$ ms^{-1} and standard lapse rates of 6.5×10^{-3} km^{-1}.

5. Concluding remarks

The main results in the investigation are those related to the three level model which is the minimum model permitting vertical variations of the static stability parameter and deviations from a linear windprofile in the basic state. As in part I the main distinctions are between sloping and non-sloping waves, where the former correspond to truly baroclinic waves.

In our examples we have concentrated on cases in which the lapse rates in the upper and lower layers are identical and equal to 6.5×10^{-3} km^{-1}. It is known (Wiin-Nielsen, 1989) that a three level model is quite sensitive to these lapse rates, in particular if one of them should approach the adiabatic lapse-rate. Such a stratification is not typical of the normal basic states, but they may occur in special circumstances, when the lower layer is modified rapidly by air-sea interaction processes as it happens when an arctic airmass moves out over a relatively warm ocean. It turns out that when γ_B is close to the adiabatic lapse rate one finds a new region of sloping baroclinic waves with a wavelength of maximum amplification of a few hundred kilometers. These cases are important in connection with the formation of the so-called polar lows, and the behavior of the three-level model in the extreme situations is described in the paper cited above.

In the more normal cases, treated here, we find for a linear profile of the basic current in the vertical direction that the stable states for the structure of the sloping waves have a westward slope, while the unstable steady states slope eastward with height. These results were expected as a natural extension of the two-level case. However, deviations from a linear profile of the wind in the basic state changes the stability in such a way that an increasing negative windshear in the upper layer will eventually destabilize the computed steady state as described in section 4 containing the results. It is also found that the three-level model gives a region of stable sloping waves of a long wavelength, but these waves do not have a westward slope in all cases.

While the methodology in this paper by and large is the same as in I it has been found that the calculations go a little easier if the relative amplitude and the relative phase are expressed as a complex number. The recent discovery has made it possible to treat the two-level case again in a brief manner (section 2).

6. Acknowledgements

Miss Kirsten Cornett has typed the manuscript and drawn the figures. The author expresses his appreciation for these timeconsuming efforts.

REFERENCES

Charney, J. G. and N. A. Phillips, 1953. Numerical integration of the quasi-geostrophic equations for barotropic and simple baroclinic flows. *J. of Meteor.*, **10**, 71-99.

Cressman, G. P., 1961. A diagnostic study of a mid-tropospheric development. *Mon. Wea. Rev.*, **89**, 74-82.

Jacobs, S. J. and A. Wiin-Nielsen, 1966. On the stability of a barotropic basic flow in a stratified atmosphere. *J. of Atmos. Sci.*, **23**, 682-687.

Wiin-Nielsen, A., 1961. Diagnosis of divergence in a three-parameter numerical prediction model. *Mon. Wea. Rev.*, **89**, 67-73.

Wiin-Nielsen, A., 1989. On the structure of transient atmospheric waves, Part I. *Atmósfera*, **2**, 3-15.

Wiin-Nielsen A., 1989. On the precursors of polar lows, Proc. of Conf. on Polar Lows, Madison, Wisc., March 1988 (to be published).